water

MDPI

Article

Baseflow from Snow and Rain in Mountain Watersheds

Helen Flynn [1,2,3], Steven R. Fassnacht [1,4,5,6,*], Marin S. MacDonald [1] and Anna K. D. Pfohl [1]

[1] ESS-Watershed Science, Colorado State University, Fort Collins, CO 80523-1476, USA; helen.flynn@colostate.edu (H.F.); marin.macdonald@colostate.edu (M.S.M.)
[2] Instituto Pirenaico de Ecología, Spanish National Research Council (IPE-CSIC), 50059 Zaragoza, Spain
[3] Geosciences, Colorado State University, Fort Collins, CO 80523-1482, USA
[4] Cooperative Institute for Research in the Atmosphere, Colorado State University, Fort Collins, CO 80523-1375, USA
[5] Instituto Geológico y Minero de España, Spanish National Research Council (IGME-CSIC), 18001 Granada, Spain
[6] Teleamb Lab, Universidad de Playa Ancha (UPLA), Playa Ancha, Valparaíso 2360004, Chile
* Correspondence: steven.fassnacht@colostate.edu

Abstract: After peak snowmelt, baseflow is the primary contributor to streamflow in snow-dominated watersheds. These low flows provide important water for municipal, agricultural, and recreational purposes once peak flows have been allocated. This study examines the correlation between peak snow water equivalent (SWE), post-peak SWE precipitation, and baseflow characteristics, including any yearly lag in baseflow. To reflect the hydrologic processes that are occurring in snow-dominated watersheds, we propose using a melt year (MY) beginning with the onset of snowmelt contributions (the first deviation from baseflow) and ending with the onset of the following year's snowmelt contributions. We identified the beginning of an MY and extracted the subsequent baseflow values using flow duration curves (FDCs) for 12 watersheds of varying sizes across Colorado, USA. Based on the findings, peak SWE and summer rain both dictate baseflow, especially for the larger watersheds evaluated, as identified by higher correlations with the MY-derived baseflow. Lags in the correlation between baseflow and peak SWE are best identified when low-snow years are investigated separately from high-snow years. The MY is a different and more effective approach to calculating baseflow using FDCs in snow-dominated watersheds in Colorado.

Keywords: baseflow; peak SWE; precipitation during snowmelt; summer rain; Colorado

Citation: Flynn, H.; Fassnacht, S.R.; MacDonald, M.S.; Pfohl, A.K.D. Baseflow from Snow and Rain in Mountain Watersheds. *Water* **2024**, *16*, 1665. https://doi.org/10.3390/w16121665

Academic Editors: Jueyi Sui and Yuntong She

Received: 6 May 2024
Revised: 5 June 2024
Accepted: 7 June 2024
Published: 12 June 2024

1. Introduction

In high-elevation, snow-dominated watersheds, baseflow is the primary driver of streamflow for most of the year, except in spring and early summer during the snowmelt season (Figures 1 and A1) when higher temperatures and increased solar radiation drive the onset of snowmelt. In such small watersheds, baseflow can persist for more than 200 days (Figure A1a,b), contributing 5 to 20% of total flow during the snow accumulation period (Figure A1c). In large catchments of the Upper Colorado River Basin, baseflow has been estimated to contribute between 40 and 86% of streamflow during low-flow periods [1]. Baseflow has been approximated using chemical mass balance hydrograph separation, frequency analysis, flow duration curves (FDCs), and tracing the movement of stable isotopes using specific conductance [2,3]. Another common method is to use a minimum of the several-day running median as a baseflow proxy [4–6]. These more complex techniques, though robust, require additional resources in the form of time and financial support, neither of which were available for this multi-decadal study. Here, we used FDCs to estimate baseflow for a time series assessment. FDCs provide a computationally inexpensive and efficient way to estimate baseflow. However, the use of FDCs in the context of the traditional water year may result in baseflow values being pulled from both before and after the peak in the hydrograph (Figure 1). In high-elevation, snow-dominated

basins, baseflow follows melt and should not be derived from the period before the peak in streamflow due to melt.

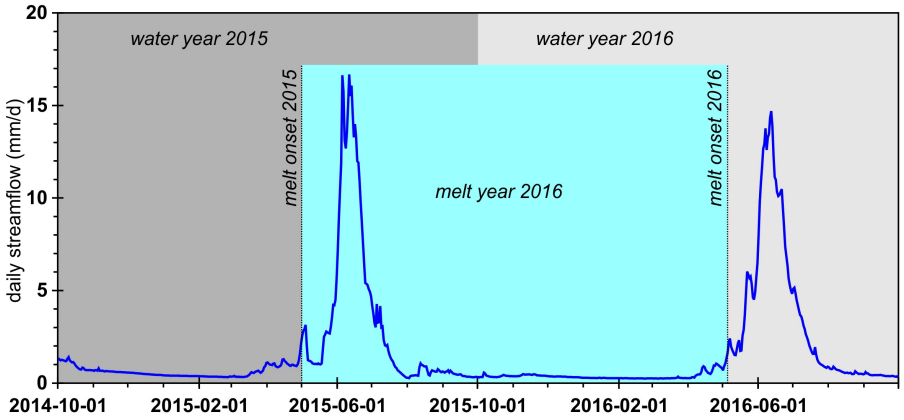

Figure 1. A sample hydrograph from the Cabin Creek gauging station illustrating two traditional water years (WYs) and a melt year as proposed in this study (MY). The MY begins with the onset of melt on 1 May 2015, and it ends one day before the next onset of melt on 5 May 2016.

While today there are a variety of techniques to measure different snowpack variables [7,8], most are newer and are not available for long historical time series. Thus, in many previous studies, the 1 April snow water equivalent (SWE) is used as a proxy for winter precipitation [9–14] due to the long record of manual, monthly snow course SWE measurements [15] and the ease of manipulation of a static date. Yet these quantities do not represent peak SWE due to their timing [16] or are not actually measured on the first of the month [17,18].

Although the relationship between winter snowpack and baseflow has been studied [4,5,19–22], the findings vary across regions, and research in Colorado using the following methods has not been conducted previously. Given that a majority of annual precipitation falls as snow in these watersheds (Figure 2), we hypothesize that peak SWE will be an indicator of baseflow volume following melt. We use FDCs to estimate baseflow and peak SWE for 12 snow-dominated watersheds in Colorado and define the following research objectives: (1) compare FDC-derived baseflow for two temporal approaches (water year versus melt year), (2) to determine the drives of baseflow, correlate peak SWE, precipitation during snowmelt, and summer precipitation with subsequent baseflow, (3) use multivariate regressions with peak SWE, precipitation during melt, summer precipitation, and baseflow derived from the melt year, and (4) correlate peak SWE and baseflow using a yearly lag from 0 to 5 years, contrasting low- and high-snow years. Throughout this study, we considered the potential implications of varying elevation, drainage area, and latitude.

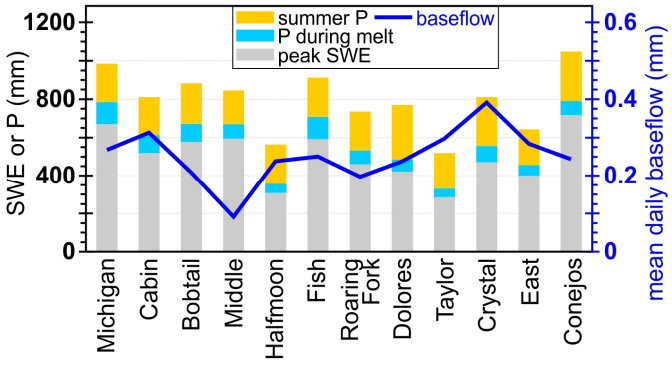

Figure 2. Mean annual peak SWE (gray), precipitation during melt (light blue), and summer precipitation (orange) in stacked bars for each station. Mean daily baseflow is represented by the blue line for each station.

2. Data

We examined streamflow, snow water equivalent, and precipitation at 12 locations for 44 years across the Rocky Mountains of Colorado, U.S.A. (Table 1 and Figure A4). We assumed that 100% of low flow was baseflow. During the cold season (approximately October through April), high elevations tend to receive larger amounts of precipitation (as snow) than lower elevations, which receive less precipitation in general, although this varies by year and location [23]. Between accumulation in the fall and the onset of melt in the spring, we assumed that no precipitation or snowmelt was contributing to runoff. We examined the period from 1 October 1979 to 30 September 2023. Daily streamflow data were obtained from the U.S. Geological Survey [24]. Stations were selected to include basins with varying drainage area, elevation, and latitudes, and all had fewer than ten years of missing data during the study period. The drainage basins that contain each stream gauge vary in latitude (37.054 to 40.496° north), elevation (2100 to 3180 m) and area (4 to 730 km^2) (Table 1 and Figure A4). Each stream gauge was paired with a U.S. Natural Resources Conservation Service (NRCS) Snow Telemetry (SNOTEL) monitoring site within or near the drainage basin (Table 1) [25]. When the nearest SNOTEL station was inactive for more than 4 consecutive years, another nearby station was selected from the same cluster based on the clusters defined by Fassnacht and Derry [26]. The peak SWE, the amount of precipitation during melt, and summer precipitation were extracted for each SNOTEL station, for each year. This precipitation during melt is on average 10 to 20% of peak SWE (Figure 2). The computed summer precipitation accounts for about 32 to 76% of peak SWE (Figure 2). The highest area of each basin is in the alpine (Table 1 and Figure A4), with the remainder of each basin being in the evergreen forest; the higher-elevation forests consist mainly of Engelmann Spruce (*Picea engelmannii*) and sub-alpine Fir (*Abies lasiocarpa*), while the lower-elevation forests consist mainly of Lodgepole Pine (*Pinus contorta*). The lowest elevations of Fish Creek and Crystal River consist of Ponderosa Pine (*Pinus ponderosa*).

Table 1. Summary of the study sites, presenting the streamflow (USGS)-paired snow (SNOTEL) stations ordered by area, with the station pair name underlined.

USGS Streamflow Gauging Station					SNOTEL Snow Station		
Code	Name	Latitude (N), Longitude (W)	Elev. (m)	Drainage Area (km^2)	Code	Name	Elev. (m)
6614800	Michigan River near Cameron Pass	40.496, 105.865	3167	3.99	551	Joe Wright	3084
9032100	Cabin Creek near Fraser	39.986, 105.745	2914	12.6	838	University Camp	3139
9034900	Bobtail Creek near Jones Pass	39.760, 105.906	3179	14.5	335	Berthoud Summit	3445
9066300	Middle Creek near Minturn	39.646, 106.382	2499	15.4	842	Vail Mountain	3139
7083000	Halfmoon Creek near Malta	39.172, 106.389	2996	60.9	369	Brumley	3231
9238900	Fish Creek near Steamboat Springs	40.475, 106.787	2179	66.3	457	Dry Lake	2560
9073300	Roaring Fork River near Aspen	39.141, 106.774	2475	196	542	Independence Pass	3231
9165000	Dolores River below Rico	37.639, 108.060	2567	275	586	Lizard Head Pass	3109
9107000	Taylor River at Taylor Park	38.860, 106.567	2847	332	680	Park Cone	2926
9081600	Crystal River near Redstone	39.233, 107.228	2105	433	618	McClure Pass	2895
9112200	East River near Crested Butte	38.784, 106.871	2573	619	380	Butte	3097
8246500	Conejos River near Mogote	37.054, 106.188	2522	730	431	Cumbres Trestle	3060

3. Methods

The traditional WY separates baseflow into two different periods (grey in Figure 1). To reflect the hydrologic processes that are occurring in snow-dominated watersheds [27], we propose using a melt year (MY) beginning with the onset of snowmelt and ending with the onset of the following year's snowmelt (Figure 1). The beginning of the MY was defined as the day at which the rate of increase in streamflow changes, defined from a specific increase in the cumulative streamflow, as presented by Pfohl and Fassnacht [28].

To find the onset of melt, the cumulative sum of the runoff was calculated for each water year. Using the cumulative sum, the onset of melt was selected as the first day when the daily slope was K times greater than the baseflow slope [28]. The constant K was determined to be 6 after testing other values to ensure that an onset of melt contributions date was selected at a reasonable time, based on manual identification of the onset of melt.

The baseflow slope was calculated between 1 January and 31 March. If the onset of melt contributions date was not identified by the routine, the MY start was manually extracted.

Once the MY was identified for each year, all daily flows in a melt year were ranked, and the probability of exceedance for each streamflow value was found; the same was performed for the 365 or 366 daily streamflow values for each WY. Flow duration curves (FDC) were constructed by plotting streamflow versus the probability of exceedance for each value per year (Figures 3 and A1b). The mean streamflow within 50–90% probability was deemed to be the annual average baseflow [2] (Figure 3). We used the Pearson correlation coefficient to compare the WY and MY average baseflow from the same year.

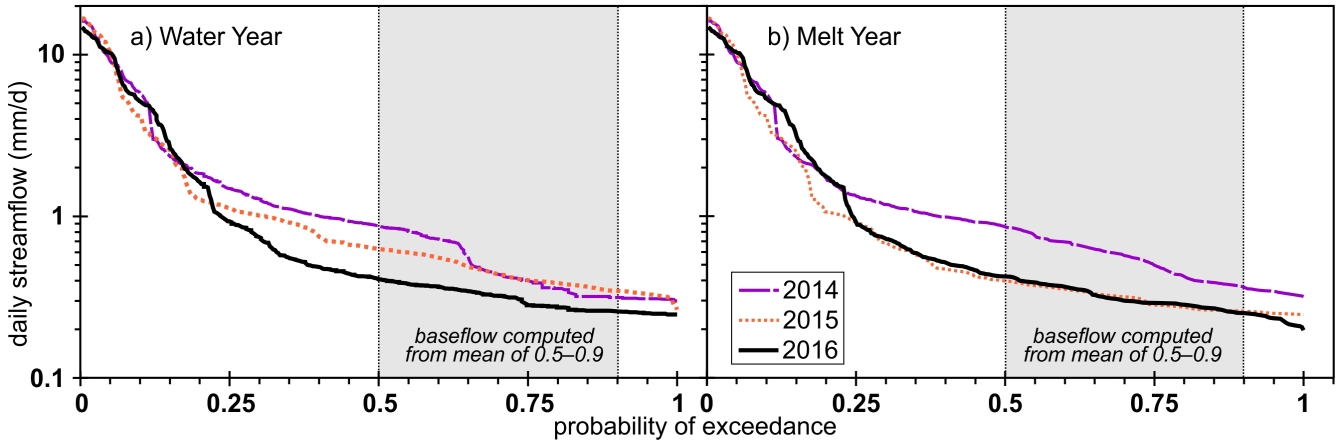

Figure 3. Flow duration curves (FDCs) from (**a**) water years (WY) and (**b**) melt years (MY) 2014, 2015, and 2016 at the Cabin stream station. Baseflow is isolated in gray.

Annual peak SWE was extracted for each station and year as the maximum SWE. Peak SWE was then correlated with the annual average baseflow values from the WY and from the same MY for all stations throughout the time series. We also correlated average WY and MY baseflow with precipitation that occurred during melt (between peak SWE and snow-all-gone) and with precipitation that occurred during the summer (after snow-all-gone and before first accumulation the following season) using Pearson's method for both.

To examine how each of these different precipitation types correlated to the MY average baseflow, multivariate regressions were run for MY baseflow versus peak SWE, precipitation during melt, and summer precipitation for each station. MY baseflow was also regressed with the sum of peak SWE and precipitation during melt, or the input from the snowpack, and summer precipitation. In each station regression, each independent variable (peak SWE, precipitation during melt, summer precipitation) for each year was divided by the maximum recorded value to standardize the independent variables to a value between 0 and 1 so that the relative regression coefficient could be compared. The correlation coefficients and p-values were also computed for each of the regressions and the latter for each independent variable in the regression.

The average MY baseflow values were correlated with peak SWE from the same year and every year prior up to 5 years using Pearson's method. For example, the MY 1985 average baseflow was compared to the peak SWE from MY 1980 (lag of 5 years) to 1985 (lag of 0 years). In addition, the peak SWE values were divided into low-, average-, and high-snow years by considering $+/-0.5$ standard deviations from the mean (approximately 30.9%) (Figure A2). We used drainage area, elevation, and latitude to compare how basin characteristics affected the results of the correlations and multivariate regressions.

4. Results

4.1. Water Year and Melt Year versus Precipitation

The MY and WY average baseflow correlation coefficient was less than 0.5 at every station, i.e., less than 50% of the variance is explained, except for Middle, which had an explained variance of 55 percent (Figure 4). Out of the 12 stations, 4 had a correlation value between the MY and WY average baseflow that was 0.3 or greater: Dolores (0.34), Roaring Fork (0.43), Conejos (0.43), and Crystal (0.48) (Figure 4). Summer precipitation and peak SWE tended to be more positively correlated with the MY average baseflow, while correlations between the WY and any of the three precipitation types were generally much smaller (Figure 4). None of the stations demonstrated a correlation between the WY average baseflow and precipitation above 0.3. The maximum R^2 value for the WY was 0.21 for the correlation between the WY average baseflow and peak SWE. Contrastingly, the correlation between the MY and summer precipitation was above 0.3 at three stations: Dolores (0.33), Crystal (0.33), and Fish (0.45). The only station that demonstrated a positive correlation between the MY average baseflow and peak SWE was Middle, with an R^2 value of 0.41. Precipitation during melt was strongly correlated with neither the MY nor the WY average baseflow.

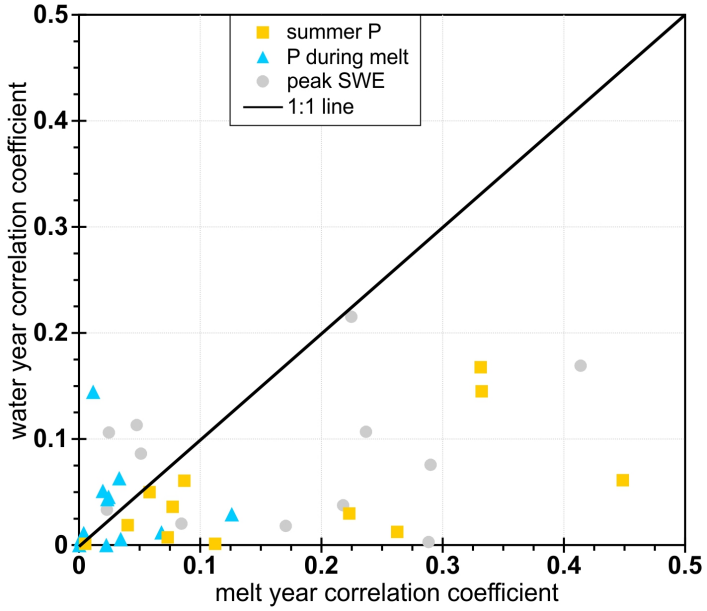

Figure 4. Comparison of the water year (WY) correlation coefficient versus the melt year (MY) correlation coefficient for the annual peak SWE (gray), precipitation during melt (light blue), and summer precipitation (orange). Only the two MY correlation coefficients greater than 0.4 were statistically significant at $p < 0.05$.

4.2. Multivariate Regressions

Both sets of multivariate regressions (MY average baseflow vs. peak SWE, P during melt, and summer P, and MY average baseflow vs. peak SWE + P during melt and summer P) demonstrated similar results. For this analysis, we will only include the results of the former (Figure 5). Of the 12 stations, all but 2 (Cabin and Bobtail) had significant (p-value < 0.05) correlation coefficients (Figure 5a). Michigan was the only station of those remaining with an R^2 below 0.3. Significant correlation coefficients above 0.5 were found at six of the stations: Fish (0.51), Dolores (0.53), Middle (0.54), East (0.55), Conejos (0.60), and Crystal (0.62) (Figure 5a). Most of the stations showed a significant relationship between both the peak SWE and summer precipitation coefficients (Figure 5b). Cabin and Bobtail were, again, the only two stations with no significant coefficients. The only time that precipitation during melt was moderately significant (p-value < 0.1) was at the Halfmoon station.

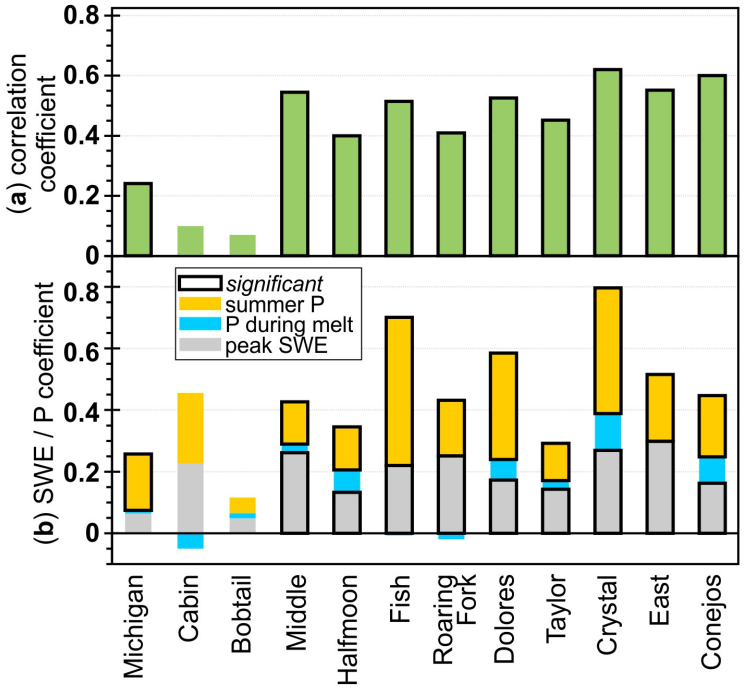

Figure 5. (**a**) Correlation coefficient and (**b**) multi-variate regression coefficients in the multi-variate regression. The solid line around a bar represents a significance of $p < 0.05$.

4.3. Melt Year versus Lagged Peak SWE

Across all years at all stations, every station had a positive R value for the comparison between the MY average baseflow and peak SWE with a lag of 0 years (Figure 6). Six had a coefficient of determination greater than 0.3, and two were greater than 0.5 across all years: Roaring Fork (0.39), Cabin (0.40), Conejos (0.40), Crystal (0.40), Halfmoon (0.41), East (0.43), Taylor (0.53), and Middle (0.55). When separated into high- and low-snow years, the low years showed a similar pattern with higher coefficients of determination at eight stations: Roaring Fork (0.39), Fish (0.51), Dolores (0.54), Cabin (0.58), Conejos (0.59), Halfmoon (0.69), Middle (0.71), and East (0.80). The other lags for the low-snow years showed inconsistent results with minimal large (greater than 0.3) coefficients of determination (Figure 6). When separated into high-snow years only, the coefficients of determination were also widely varied, with four stations having a more negative value at lag 0 (Middle, Dolores, Taylor, and East), while Cabin demonstrated a large positive value (0.46) (Figure 6). There were two stations for lag 1 with coefficients of determination larger than 0.3, and two more with values larger than 0.5: Dolores (0.32), Roaring Fork (0.45), Middle (0.51), and Fish (0.51). The two stations that had lag 0 values less than –0.3 and lag 1, 2, and 3 values greater than 0.3 were Middle and Dolores (the latter also had a lag 4 coefficient of determination of 0.56) (Figure 6).

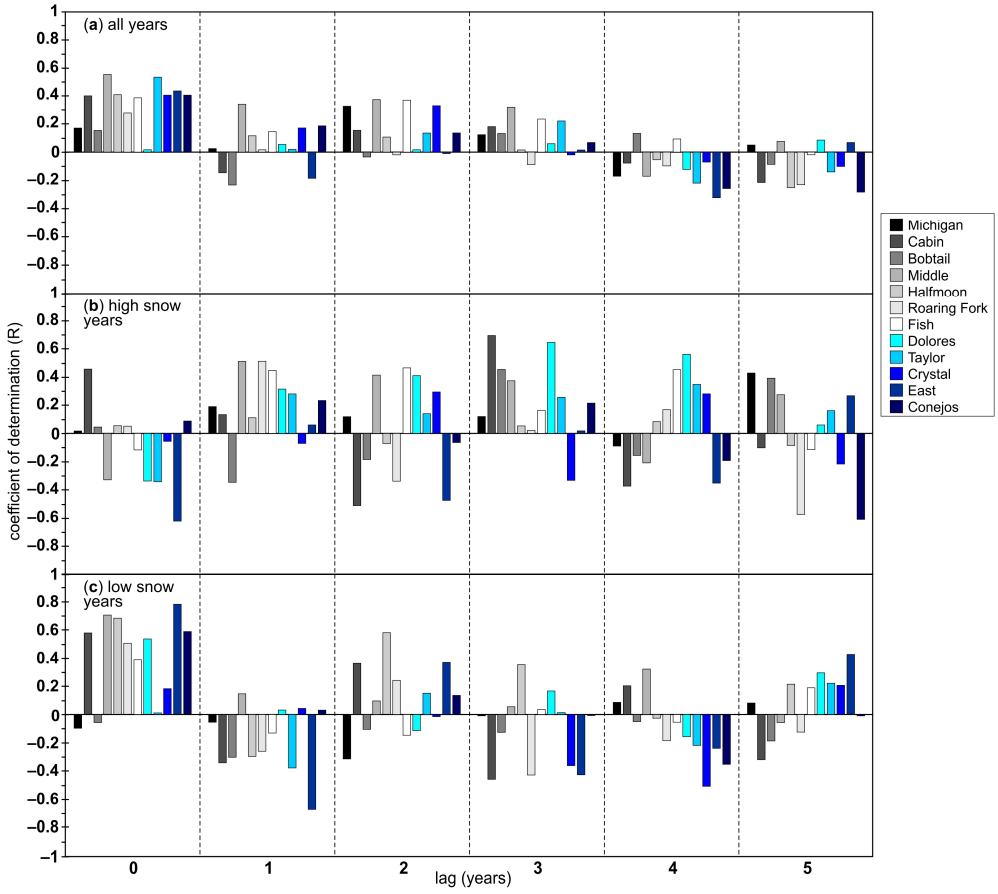

Figure 6. Coefficient of determination for each station with lag from 0 to 5 years for (**a**) all years, (**b**) high-snow years, and (**c**) low-snow years.

5. Discussion

Most of the stations (8 out of 12) showed a very weak correlation between the MY and WY average baseflow (e.g., Figure 3). This indicates that deriving baseflow from FDCs with the MY approach produces different (Figure 4) and more representative baseflow values than using the traditional WY. The larger-drainage-area basins showed a slightly higher correlation between the MY and WY average baseflow. This could indicate that larger basins are less likely to experience high amounts of interannual variability in baseflow (Figure A3), and thus more similar MY and WY baseflow values. The larger basin size could also act as a buffer to interannual variability in peak SWE and subsequent baseflow [29].

The correlation between the MY, WY, and precipitation types shows a stronger connection between the MY average baseflow and both peak SWE and summer precipitation (Figure 4). Because neither the MY nor the WY average baseflow was highly correlated with precipitation during melt, it can be assumed that precipitation during this time does not have as big of an impact on baseflow as other forms of precipitation. Precipitation during snowmelt tends to be small compared to snowfall prior, i.e., peak SWE (Figure 2), but, like SWE (Figure A2), it does vary interannually [30].

Similarly, peak SWE and summer precipitation tended to have more significant correlations to the MY average baseflow in the multivariate regressions. While precipitation during melt contributes less water to baseflow than the snowpack and summer precipitation, these values were standardized to ensure that the differences in magnitude of the precipitation types were not influencing the correlations and, thus, it can be assumed that precipitation during melt is less correlated with baseflow than the other two precipitation groups. This could have implications for water availability in the face of climate change, as timing and quantity of precipitation are changing [31–33].

Since peak SWE showed a larger correlation to the MY average baseflow values in the direct correlation (Figure 4) and the multivariate regressions (Figure 5), it is expected to see the same results for a lag of 0 years. The low-snow years seemed to directly impact the baseflow values during the same year but not years later, which is likely due to the interannual variability of peak SWE in the basins (Figure 6c). During high-snow years, where there do not appear to be many high coefficients of determination (Figure 6b), it is possible that the excess runoff replenished depleted groundwater supplies from low years but did not lead to a legacy effect increase like that explored by Godsey et al. [4]. The variable nature of the snowpack in these basins likely acts as a buffer to impacts of low- and high-snow years beyond the subsequent baseflow from the same year.

As in this study, baseflow is often estimated through separation of the other main component of streamflow, runoff, using various methods. Some techniques used to estimate baseflow include baseflow separation using recession analysis [34], the chemical hydrograph separation approach [3], the minimum 7-day moving average [5], and conductivity–mass–balance hydrograph separation [21,35,36]. Here, we used FDCs [2] (Figure 2). For the small headwater basins examined in this study (Table 1, Figure A4), the snowpack does not begin to melt until after peak accumulation (Figure 3), which typically occurs in April or May [30]. While rain-on-snow is becoming more relevant in snow-dominated systems [37,38], in the watersheds that we studied, rainfall is limited [30,39]. Once the snowpack begins to accumulate in the fall, which usually begins in October, there are seven or eight months of the year with no precipitation or snowmelt input into the streamflow [20] (Figures 1 and A1). Thus, using FDCs to identify baseflow (Figures 1 and A1) is valid. There is baseflow throughout the year (Figures 1 and A1a) [1], including during snowmelt [1,21]; here, we are focusing on the maintenance of winter low flows. Specific conductance, together with water temperature, is being added to streamflow gauging stations [3,21] and could be used to assess baseflow throughout the year as a comparison to the FDC approach used herein. However, variation in specific conductance does not always indicate baseflow changes [40], and detailed investigations must examine hillslope processes at various scales [41–43]. Furthermore, a changing climate will alter the timing and nature of baseflow [19,22,44–48].

One SNOTEL station was used to represent each watershed (Table 1). Point snow measurements or stations may not be representative of the area surrounding them [49,50]. However, the SNOTEL stations are an index of the snowpack [15,25,49] and represent the interannual variability of the snowpack (Figure A2), which tends to be spatially consistent [51]. Using multiple snow stations could better identify the actual amount of snow [7], but this current paper focuses on the correlation between snow, rain (Figure 3), and baseflow (Figures 4 and 5), as well as the lags between them (Figure 6).

6. Conclusions

The use of the MY, i.e., starting at the rise of the hydrograph at the onset of snowmelt contributions, is a novel approach to calculating baseflow in small, snow-dominated watersheds. The MY baseflow amounts are a more accurate representation of baseflow as a product of snowmelt and are different from WY average baseflow amounts. Peak SWE and summer precipitation have the largest impact on the resulting MY baseflow during the same year, but precipitation during melt does not correlate highly with MY average baseflow. Both the simple correlations and multivariate regressions showed that baseflow derived from FDCs using the MY rather than the WY more accurately represents the hydrological processes occurring in high-elevation, snow-dominated watersheds in Colorado. Future research could include the use of triple diagram models to examine the influence of climate on peak SWE and baseflow, as well as a more in-depth examination of the influence of basin characteristics.

Author Contributions: Conceptualization, S.R.F., H.F., M.S.M. and A.K.D.P.; methodology, H.F., S.R.F., M.S.M. and A.K.D.P.; software, H.F., M.S.M. and A.K.D.P.; formal analysis, H.F., S.R.F. and M.S.M.; investigation, H.F., S.R.F., M.S.M. and A.K.D.P.; data curation, H.F. and M.S.M.; writing—

original draft preparation, H.F., S.R.F. and M.S.M.; writing—review and editing, H.F., S.R.F., M.S.M. and A.K.D.P.; visualization, S.R.F. and H.F.; supervision, S.R.F. and A.K.D.P.; project administration, S.R.F. All authors have read and agreed to the published version of the manuscript.

Funding: This research received no external funding.

Data Availability Statement: These data were derived from the following resources available in the public domain: http://waterdata.usgs.gov/nwis/, https://www.nrcs.usda.gov/ (accessed 6 June 2024).

Acknowledgments: We would like to thank Matthew Ross of Colorado State University for his guidance and support with managing the data. H.F. and S.R.F. both thank the Fulbright Program and Fulbright España for all other support. S.R.F. also thanks Fulbright Chile.

Conflicts of Interest: The authors declare no conflicts of interest.

Appendix A. Interannual Variability of Streamflow and Peak SWE

This appendix provides a station example of streamflow over the study period as daily hydrographs starting at the onset of melt (Figure A1a) and ranked per MY (Figure A1b) and the 43-year time series of total runoff and the runoff during flow snowpack accumulation (Figure A1c). An example is presented for a peak SWE time series (Figure A2).

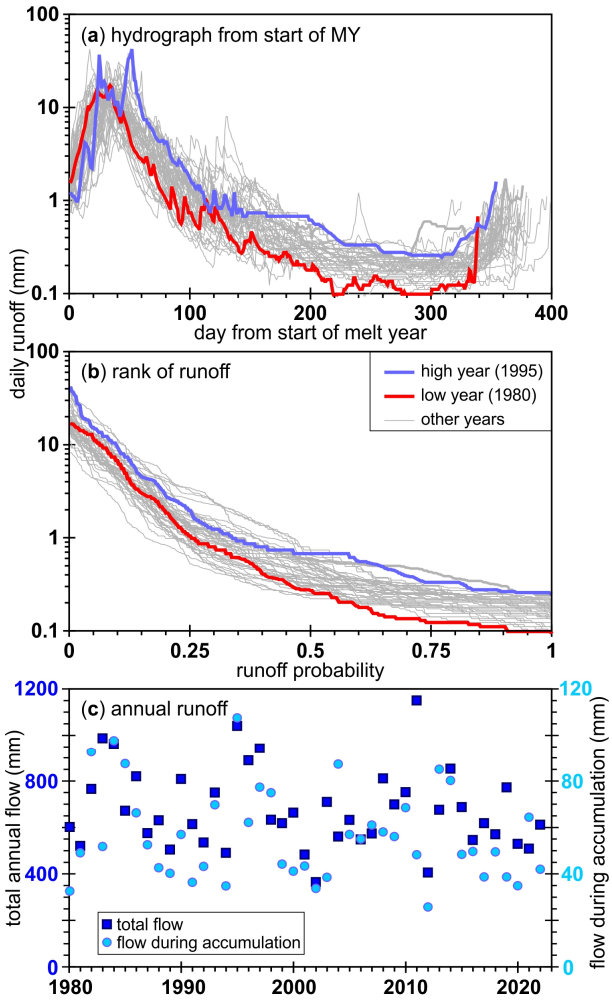

Figure A1. Example of interannual variability among (**a**) streamflow hydrographs, (**b**) ranked runoff for the Michigan River streamflow gauging station from 1980 to 2022 with a low (1980) and high (1995) flow year identified, and (**c**) annual time series of total runoff (dark blue) and runoff during snow accumulation (light blue).

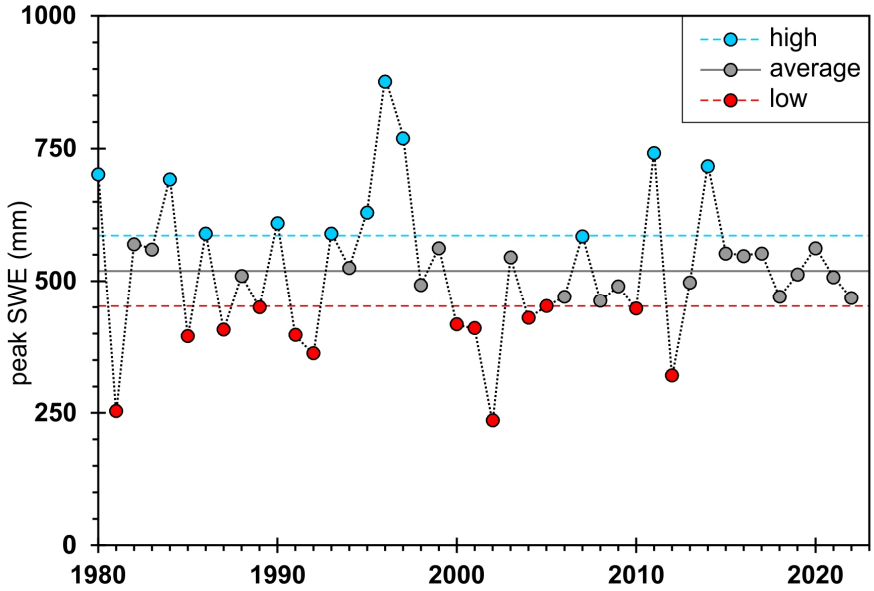

Figure A2. Example of interannual variability of peak SWE at Cabin Creek SNOTEL station from 1980 to 2022 with peak SWE separated into low, average, and high years using 0.5 standard deviations from the mean of the time series.

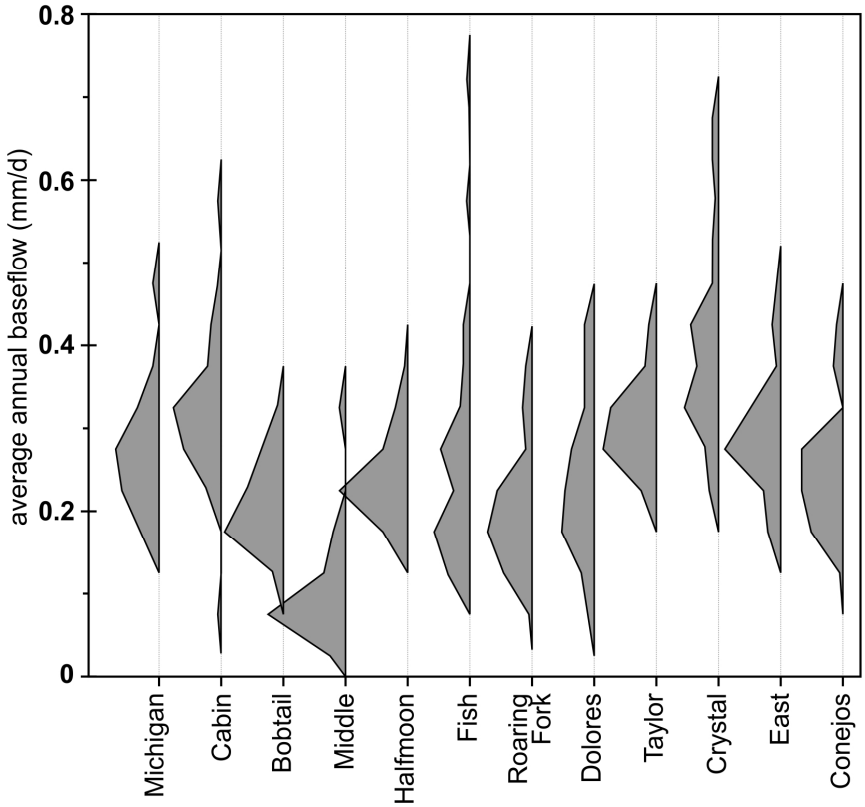

Figure A3. The variation in average baseflow for the 12 stations examined in this study in order of basin size from least to greatest [52].

Appendix B. Location Map

This appendix presents a location map for the 12 study watersheds, plus their shape, relative size, and general orientation (Figure A4).

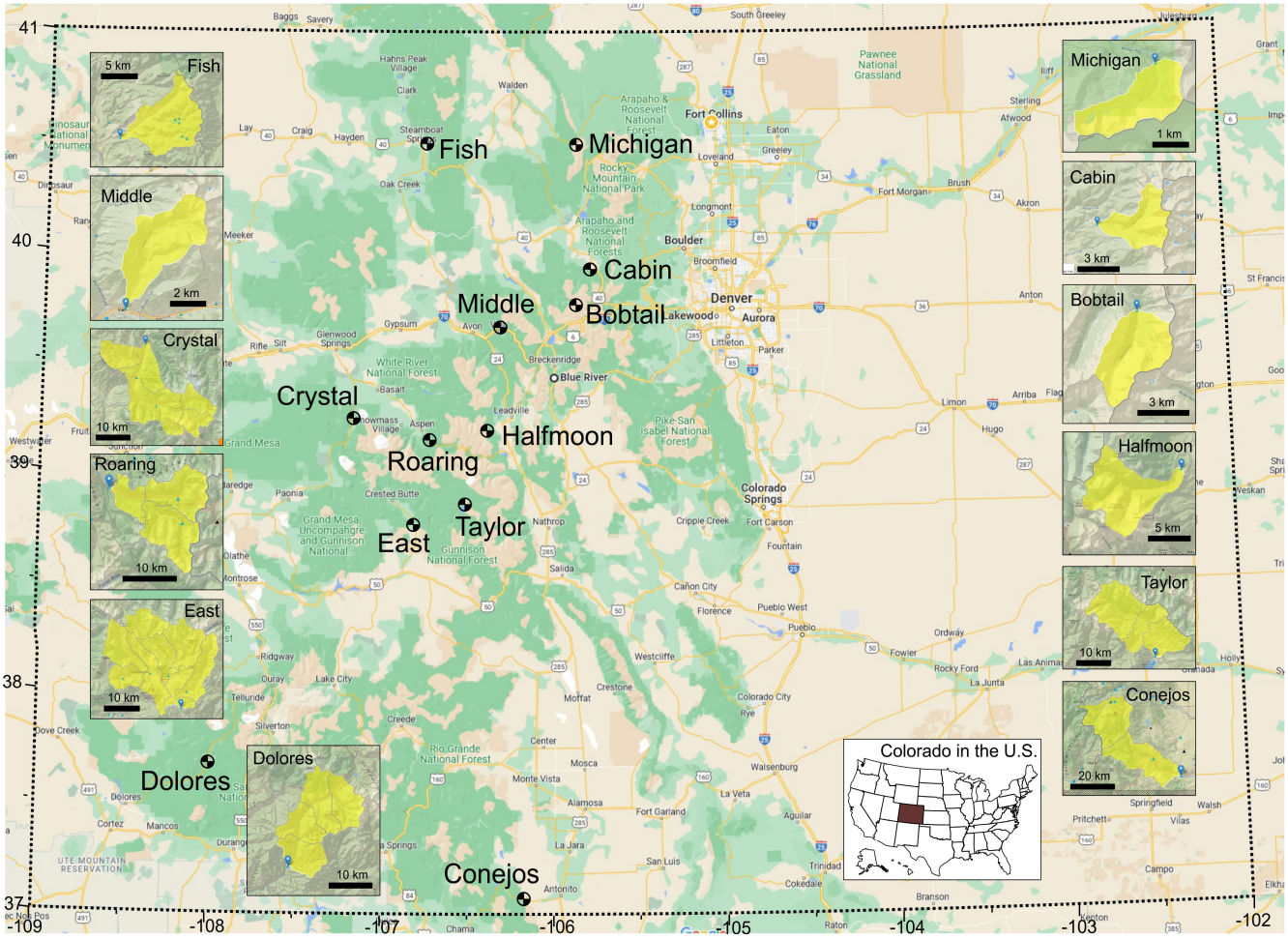

Figure A4. Location map of the 12 study watersheds in the state of Colorado, U.S.A. (inset) illustrating the shape of each watershed.

References

1. Miller, M.P.; Buto, S.G.; Susong, D.D.; Rumsey, C.A. The Importance of Base Flow in Sustaining Surface Water Flow in the Upper Colorado River Basin. *Water Resour. Res.* **2016**, *52*, 3547–3562. [CrossRef]
2. Smakhtin, V.U. Low Flow Hydrology: A Review. *J. Hydrol.* **2001**, *240*, 147–186. [CrossRef]
3. Miller, M.P.; Susong, D.D.; Shope, C.L.; Heilweil, V.M.; Stolp, B.J. Continuous Estimation of Baseflow in Snowmelt-dominated Streams and Rivers in the Upper Colorado River Basin: A Chemical Hydrograph Separation Approach. *Water Resour. Res.* **2014**, *50*, 6986–6999. [CrossRef]
4. Godsey, S.E.; Kirchner, J.W.; Tague, C.L. Effects of Changes in Winter Snowpacks on Summer Low Flows: Case Studies in the Sierra Nevada, California, USA. *Hydrol. Process.* **2014**, *28*, 5048–5064. [CrossRef]
5. Jenicek, M.; Seibert, J.; Zappa, M.; Staudinger, M.; Jonas, T. Importance of Maximum Snow Accumulation for Summer Low Flows in Humid Catchments. *Hydrol. Earth Syst. Sci.* **2016**, *20*, 859–874. [CrossRef]
6. Cooper, M.G.; Schaperow, J.R.; Cooley, S.W.; Alam, S.; Smith, L.C.; Lettenmaier, D.P. Climate Elasticity of Low Flows in the Maritime Western U.S. Mountains. *Water Resour. Res.* **2018**, *54*, 5602–5619. [CrossRef]
7. Dozier, J.; Bair, E.H.; Davis, R.E. Estimating the Spatial Distribution of Snow Water Equivalent in the World's Mountains. *WIREs Water* **2016**, *3*, 461–474. [CrossRef]
8. Fassnacht, S.R. A Call for More Snow Sampling. *Geosciences* **2021**, *11*, 435. [CrossRef]
9. Cayan, D.R. Interannual Climate Variability and Snowpack in the Western United States. *J. Clim.* **1996**, *9*, 928–948. [CrossRef]
10. Serreze, M.C.; Clark, M.P.; Armstrong, R.L.; McGinnis, D.A.; Pulwarty, R.S. Characteristics of the western United States snowpack from snowpack telemetry (SNOTEL) data. *Water Resour. Res.* **1999**, *35*, 2145–2160. [CrossRef]
11. Cayan, D.R.; Kammerdiener, S.A.; Dettinger, M.D.; Caprio, J.M.; Peterson, D.H. Changes in the Onset of Spring in the Western United States. *Bull. Amer. Meteor. Soc.* **2001**, *82*, 399–416. [CrossRef]
12. Lute, A.C.; Luce, C.H. Are Model Transferability And Complexity Antithetical? Insights From Validation of a Variable-Complexity Empirical Snow Model in Space and Time. *Water Resour. Res.* **2017**, *53*, 8825–8850. [CrossRef]

13. Tamaddun, K.A.; Kalra, A.; Bernardez, M.; Ahmad, S. Multi-Scale Correlation between the Western U.S. Snow Water Equivalent and ENSO/PDO Using Wavelet Analyses. *Water Resour. Manag.* **2017**, *31*, 2745–2759. [CrossRef]
14. Brown, R.D.; Fang, B.; Mudryk, L. Update of Canadian Historical Snow Survey Data and Analysis of Snow Water Equivalent Trends, 1967–2016. *Atmos. Ocean* **2019**, *57*, 149–156. [CrossRef]
15. Natural Resource Conservation Service (NRCS). *The History of Snow Survey and Water Supply Forecasting, Interviews with U.S. Department of Agriculture Pioneers*; Helms, D., Phillips, S., Reich, P., Eds.; Natural Resources Conservation Service; U.S. Department of Agriculture, Natural Resources Conservation Service: Washington DC, USA, 2008. Available online: https://www.nrcs.usda.gov/sites/default/files/2022-09/History-Of-Snow-Survey.pdf (accessed on 8 April 2024).
16. Bohr, G.S.; Aguado, E. Use of April 1 SWE Measurements as Estimates of Peak Seasonal Snowpack and Total Cold-Season Precipitation. *Water Resour. Res.* **2001**, *37*, 51–60. [CrossRef]
17. Pagano, T.C. Quantification of the Influence of Snow Course Measurement Date on Climatic Trends. *Clim. Change* **2012**, *114*, 549–565. [CrossRef]
18. Montoya, E.L.; Dozier, J.; Meiring, W. Biases of April 1 Snow Water Equivalent Records in the Sierra Nevada and Their Associations with Large-scale Climate Indices. *Geophys. Res. Lett.* **2014**, *41*, 5912–5918. [CrossRef]
19. Dierauer, J.R.; Whitfield, P.H.; Allen, D.M. Climate Controls on Runoff and Low Flows in Mountain Catchments of Western North America. *Water Resour. Res.* **2018**, *54*, 7495–7510. [CrossRef]
20. Hammond, J.C.; Kampf, S.K. Subannual Streamflow Responses to Rainfall and Snowmelt Inputs in Snow-Dominated Watersheds of the Western United States. *Water Resour. Res.* **2020**, *56*, e2019WR026132. [CrossRef]
21. Rumsey, C.A.; Miller, M.P.; Sexstone, G.A. Relating Hydroclimatic Change to Streamflow, Baseflow, and Hydrologic Partitioning in the Upper Rio Grande Basin, 1980 to 2015. *J. Hydrol.* **2020**, *584*, 124715. [CrossRef]
22. Siirila-Woodburn, E.R.; Rhoades, A.M.; Hatchett, B.J.; Huning, L.S.; Szinai, J.; Tague, C.; Nico, P.S.; Feldman, D.R.; Jones, A.D.; Collins, W.D.; et al. A Low-to-No Snow Future and Its Impacts on Water Resources in the Western United States. *Nat. Rev. Earth Environ.* **2021**, *2*, 800–819. [CrossRef]
23. Preece, J.R.; Shinker, J.J.; Riebe, C.S.; Minckley, T.A. Elevation-Dependent Precipitation Response to El Niño-Southern Oscillation Revealed in Headwater Basins of the US Central Rocky Mountains. *Int. J. Climatol.* **2021**, *41*, 1199–1210. [CrossRef]
24. USGS National Water Information System. USGS Water Data for the Nation. Available online: http://waterdata.usgs.gov/nwis/ (accessed on 21 November 2023).
25. Natural Resources Conservation Service. Report Generator; Air and Water Database Report Generator. Available online: https://wcc.sc.egov.usda.gov/reportGenerator/ (accessed on 21 November 2023).
26. Fassnacht, S.R.; Derry, J.E. Defining Similar Regions of Snow in the Colorado River Basin Using Self-organizing Maps. *Water Resour. Res.* **2010**, *46*, 2009WR007835. [CrossRef]
27. Whitfield, P.H. Is 'Centre of Volume' a Robust Indicator of Changes in Snowmelt Timing? *Hydrol. Process.* **2013**, *27*, 2691–2698. [CrossRef]
28. Pfohl, A.K.D.; Fassnacht, S.R. Evaluating Methods of Streamflow Timing to Approximate Snowmelt Contribution in High-Elevation Mountain Watersheds. *Hydrology* **2023**, *10*, 75. [CrossRef]
29. Black, P.E. Watershed Functions. *J. Am. Water Resour. Assoc.* **1997**, *33*, 1–11. [CrossRef]
30. Fassnacht, S.; Collados-Lara, A.-J.; Xu, K.; Sears, M.; Pulido-Velazquez, D.; Morán-Tejeda, E. Defining Actual Daily Snowmelt Rates from In Situ Snow Water Equivalent Measurements. In Proceedings of the 39th IAHR World Congress; International Association for Hydro-Environment Engineering and Research (IAHR), Granada, Spain, 19–24 June 2022; pp. 260–267.
31. Trenberth, K. Changes in Precipitation with Climate Change. *Clim. Res.* **2011**, *47*, 123–138. [CrossRef]
32. Musselman, K.N.; Lehner, F.; Ikeda, K.; Clark, M.P.; Prein, A.F.; Liu, C.; Barlage, M.; Rasmussen, R. Projected Increases and Shifts in Rain-on-Snow Flood Risk over Western North America. *Nat. Clim. Change* **2018**, *8*, 808–812. [CrossRef]
33. Allan, R.P.; Barlow, M.; Byrne, M.P.; Cherchi, A.; Douville, H.; Fowler, H.J.; Gan, T.Y.; Pendergrass, A.G.; Rosenfeld, D.; Swann, A.L.S.; et al. Advances in Understanding Large-scale Responses of the Water Cycle to Climate Change. *Ann. N. Y. Acad. Sci.* **2020**, *1472*, 49–75. [CrossRef]
34. Eckhardt, K. A Comparison of Baseflow Indices, Which Were Calculated with Seven Different Baseflow Separation Methods. *J. Hydrol.* **2008**, *352*, 168–173. [CrossRef]
35. Burt, T.P. The Relationship between Throughflow Generation and the Solute Concentration of Soil and Stream Water. *Earth Surf. Process.* **1979**, *4*, 257–266. [CrossRef]
36. Matsubayashi, U.; Velasquez, G.T.; Takagi, F. Hydrograph Separation and Flow Analysis by Specific Electrical Conductance of Water. *J. Hydrol.* **1993**, *152*, 179–199. [CrossRef]
37. Il Jeong, D.; Sushama, L. Rain-on-Snow Events over North America Based on Two Canadian Regional Climate Models. *Clim. Dyn.* **2018**, *50*, 303–316. [CrossRef]
38. Würzer, S.; Jonas, T. Spatio-temporal Aspects of Snowpack Runoff Formation during Rain on Snow. *Hydrol. Process.* **2018**, *32*, 3434–3445. [CrossRef]
39. Morán-Tejeda, E.; Fassnacht, S.; Collados-Lara, A.-J.; Pfohl, A.; Tedesche, M.; Pulido-Velazquez, D. A Proposal for Studying Rain-on-Snow Events: A Case Study from SNOTEL Data in the Southern Rocky Mountains, U.S.A. In Proceedings of the 39th IAHR World Congress; International Association for Hydro-Environment Engineering and Research (IAHR), Granada, Spain, 19–24 June 2022; pp. 268–273.

40. Cartwright, I.; Miller, M.P. Temporal and Spatial Variations in River Specific Conductivity: Implications for Understanding Sources of River Water and Hydrograph Separations. *J. Hydrol.* **2021**, *593*, 125895. [CrossRef]
41. Kuraś, P.K.; Weiler, M.; Alila, Y. The Spatiotemporal Variability of Runoff Generation and Groundwater Dynamics in a Snow-Dominated Catchment. *J. Hydrol.* **2008**, *352*, 50–66. [CrossRef]
42. Jencso, K.G.; McGlynn, B.L.; Gooseff, M.N.; Bencala, K.E.; Wondzell, S.M. Hillslope Hydrologic Connectivity Controls Riparian Groundwater Turnover: Implications of Catchment Structure for Riparian Buffering and Stream Water Sources. *Water Resour. Res.* **2010**, *46*, 2009WR008818. [CrossRef]
43. Hinckley, E.S.; Ebel, B.A.; Barnes, R.T.; Anderson, R.S.; Williams, M.W.; Anderson, S.P. Aspect Control of Water Movement on Hillslopes near the Rain–Snow Transition of the Colorado Front Range. *Hydrol. Process.* **2014**, *28*, 74–85. [CrossRef]
44. Sui, K.; Koehler, G. Rain-on-snow induced flood events in southern Germany. *J. Hydrol.* **2001**, *252*, 205–220. [CrossRef]
45. Sui, K.; Koehler, G. Impacts of snowmelt on peak flows in a forest watershed. *Water Resour. Manag.* **2007**, *21*, 1263–1275. [CrossRef]
46. Jefferson, A.; Nolin, A.; Lewis, S.; Tague, C. Hydrogeologic Controls on Streamflow Sensitivity to Climate Variation. *Hydrol. Process.* **2008**, *22*, 4371–4385. [CrossRef]
47. Sui, K.; Koehler, G.; Krol, F. Characteristics of rainfall, snowmelt and runoff in the headwater region of the Main River Watershed in Germany. *Water Resour. Manag.* **2010**, *24*, 2167–2186. [CrossRef]
48. Li, D.; Wrzesien, M.L.; Durand, M.; Adam, J.; Lettenmaier, D.P. How Much Runoff Originates as Snow in the Western United States, and How Will That Change in the Future? *Geophys. Res. Lett.* **2017**, *44*, 6163–6172. [CrossRef]
49. Daly, S.F.; Davis, R.; Ochs, E.; Pangburn, T. An approach to spatially distributed snow modelling of the Sacramento and San Joaquin basins, California. *Hydrol. Process.* **2000**, *14*, 3257–3271. [CrossRef]
50. Meromy, L.; Molotch, N.P.; Link, T.E.; Fassnacht, S.R.; Rice, R. Subgrid Variability of Snow Water Equivalent at Operational Snow Stations in the Western USA. *Hydrol. Process.* **2013**, *27*, 2383–2400. [CrossRef]
51. Sturm, M.; Wagner, A.M. Using Repeated Patterns in Snow Distribution Modeling: An Arctic Example. *Water Resour. Res.* **2010**, *46*, 2010WR009434. [CrossRef]
52. Curtis, I.; Hook, P.; Sumner, B.; Morris, S. Disorder. In *Unknown Pleasures*; Factory: Manchester, UK, 1979; Chapter 1.